

An Improved Predesign Procedure for Shaped-Beam Reflectarrays

Jianfeng Yu^{*}, Lei Chen, Jing Yang, and Xiaowei Shi

Abstract—This article describes an improved design procedure for shaped-beam reflectarrays, which is advanced mainly in accuracy and concision. Specifically, the excitation has been computed by a new approach named local simulation instead of mathematical modeling, which demonstrates more advantage in precision. The intersection approach has been applied to optimization, and it is improved by introducing a new multi-stage strategy into the synthesis process to avoid local minima. Moreover, the phase-only optimization, calculation of the reflection phase data table and the simulation verification processes are combined as a co-simulation procedure by VBScript (Visual Basic Script). This procedure is very beneficial to design reflectarrays with efficiency. As an example, a reflectarray consists of 621 dual-loop elements is optimized, and a good sectored-cosecant squared beam result is obtained.

1. INTRODUCTION

Flat printed reflectarrays, containing advantageous features of reflectors and regular microstrip arrays, such as low cost, high gain, simple manufacture process and suitability for beam shaping, have been extensively studied during recent decades [1].

Putting cost first, the predesign is important for reflectarrays before fabrication, which includes parameters characterization and simulation verification. Plenty reported collimated-beam reflectarrays, which focus on the radiating properties such as broadband [2] and multi-band [3], are realized by improving elementary frequency characteristics. However, other than the bandwidth, array layout and reconfigurability, more efforts have been made to promote the radiating patterns for shaped-beam applications such as Local Multipoint Distribution System (LMDS) [4], Direct Broadcast Satellite (DBS) [5] and Multiple Beam Radiation (MBR) [6]. With steerable patterns and more elements, shaped-beam reflectarrays are more complex than the collimated-beam ones.

The predesign of a shaped-beam reflectarray is divided into three sections, i.e., the optimization process, calculation of the element reflecting phase data table and the simulation verification. Firstly, the alternating projection method (APM, namely, intersection approach) [7] is utilized as the optimization algorithm because of its high efficiency in solving the huge unknowns of large reflectarrays. As a local optimization algorithm, the convergence of APM is easily affected by the starting point. Nevertheless, it has been confirmed that a starting phase distribution, which generates the radiation pattern approximate to the desired shaped beam, not only helps converge, but also reduces the number of iterations directly using APM [5, 8]. Although the results met the requirements, as reported in [6], searching for the proper starting phase distribution still costs much work. Further, a several-stage phase-only synthesis technique has been proposed to avoid local minima in [9], by which the optimization process was divided into several stages. The illumination taper was increased gradually from one stage to the next, which was realized by decreasing q of the feed model function $(\cos^q \theta)$ [1]. As a result, the starting phase distribution was not as critical as the former by using this technique. It was claimed that an initial

Received 3 September 2014, Accepted 17 December 2014, Scheduled 17 December 2014

^{*} Corresponding author: Jianfeng Yu (jianf.yu88@gmail.com).

The authors are with the Science and Technology on Antenna and Microwave Laboratory, Xidian University, Xi'an, Shaanxi 710071, China.

phase distribution associated with an out of focus beam could also lead to a satisfactory pattern in [10]. However, this several-stage method, is apparently of less accuracy for predesign since itself is an ideal mathematical model. Secondly, in most literatures concentrated on reflectarray optimization [6, 11, 12], rectangular patch elements are accurately computed via Spectral Domain Method of Moments (SDMoM) considering local periodicity [13]. As the SDMoM is not suitable for non-rectangular patches, the commercial software is a good tradeoff between theoretical learning cost, complexity and consumed time for arbitrary shaped radiating elements [14]. Lastly, for the simulation verification of a large reflectarray, building a model is an urgent problem, which is time consuming since all elements differ from each other.

This article presents an improved predesign approach for shaped-beam reflectarrays. A local simulation method has been proposed for excitation calculation. The result shows more satisfactory accuracy compared with the mathematical modeling result. After that, a new multi-stage convergence strategy has been applied into the phase-only synthesis process using the excitation calculated by the local simulation method. A co-simulation approach has been achieved by combining the optimization and simulation together using VBScript. The predesign procedure is then improved with simplicity and automation. Finally, a reflectarray predesign example is presented with a simple dual-loop element for validation. The proposed strategy not only leads to the result of optimization away from local minima without the redundant feed modeling function but also makes the design process simpler, and helps generate a similar result with that in [15].

2. EXCITATION CALCULATION

The schematic of a reflectarray is shown in Figure 1, and the layout of the antenna discussed in this article is demonstrated as follows. Consider that radiating non-canonical patches with varying sizes lie uniformly ($d_x \times d_y$) on the X - Y plane, beneath which a substrate is backed by a ground plane. The feed is placed on the X - Z plane, so the vertical polarization is aligned with y axis. In this article, only vertical field is taken into account, and the horizontal one gives rise to polarization loss.

Excitation distribution illuminated on the aperture should be chiefly solved before optimization. A corrugated horn is employed as the feed in this paper. Two kinds of excitation computing approaches are compared as follows.

2.1. Mathematical Modeling Function

As aforementioned, the feed pattern is generally modeled by the q th power of a cosine function, which is specified as

$$q_{E/H} = -\frac{1}{2} \frac{\ln 2}{\ln \cos (HPBW_{E/H}/2)}, \quad (1)$$

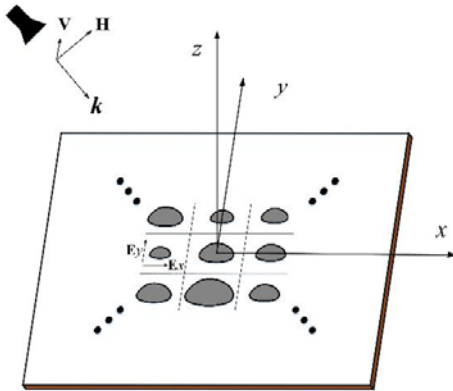


Figure 1. Geometrical model of the reflectarray with varying sized patches.

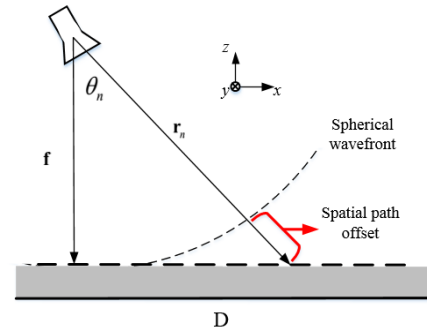


Figure 2. Scheme of compensation for space attenuation factor ($y = 0$ cut plane).

where $HPBW_{E/H}$ is short for half power beam width of E/H plane. E_x and E_y (marked out in Figure 1) are easily calculated via coordinate transformation and polarization decomposition with the pattern model function in [16]. Specifically, the employed feed is modeled as $q_E = q_H = 16.5$.

2.2. Local Simulation

An alternative way to analyze the excitation is by simulation. Here the ANSYS High Frequency Structure Simulator (HFSS) is used to solve the feed pattern. However, the computing process is time consuming if the feed antenna is simulated by full-wave analysis considering the array surface. A new approach named local simulation is proposed to address the problem, in which the feed is isolated solved. The array is assumed to locate in the Fresnel zone of the primary feed where spherical wave dominates. Therefore to obtain the field along the X - Y plane, the errors caused by spatial path offset between the spherical wave front and the aperture surface should be compensated. The compensation mechanism is illustrated in Figure 2, where f is the focal length, \mathbf{r}_{mn} is the position vector of element (m, n) , and θ_{mn} represents the angle between \mathbf{f} and \mathbf{r}_{mn} . In addition, the feed's phase center is set as the origin.

Firstly, the field at a distance of \mathbf{f} is easily solved by HFSS. It is reasonable to consider the electric field of the feed proportional to $1/r$ since $1/r^2$ and the higher order ones negligible in the Fresnel zone. For the (m, n) th element, the concerned amplitude of incidence has the relationship given by

$$\left| \mathbf{E}_{V/H}^{\mathbf{r}_{mn}} \right| \propto \frac{1}{r_{mn}}. \quad (2)$$

Secondly, compared to the already known field at the radius of f , the field on the planar aperture is solved by compensation. Due to $r_{mn} = f / \cos \theta_{mn}$, (2) is derived in dB as

$$\left| \mathbf{E}_{V/H}^{\mathbf{r}_{mn}} \right|_{\text{dB}} \propto 20 \lg \left(\frac{1}{f} \right) + 20 \lg (\cos \theta_{mn}) \quad (3)$$

Obviously, the first term on the right side of (3) is related to the simulated spherical wave front, and the latter is the Space Power Attenuation Factor (SPAF), similar to that of parabolic reflectors. Equation (3) indicates higher space loss comes with larger incident angle θ_{mn} . Simultaneously, the phase variation, caused by the spatial path offset, should also be compensated. Derived from $|\mathbf{r}_{mn}| - |\mathbf{f}|$, the phase of incident wave $\Phi_{V/H}^{\mathbf{r}_{mn}}$ at (m, n) th element is given by

$$\Phi_{V/H}^{\mathbf{r}_{mn}} = \Phi_{V/H}^{\mathbf{f}} + (|\mathbf{r}_{mn}| - |\mathbf{f}|) / \lambda, \quad (4)$$

which has been widely applied in the collimated-beam reflectarray designs as the ray tracing method.

In brief, the sequence of solving the electric field on the array surface through HFSS is as follows. Starting with searching the phase center of the feed, the field at a distance of f is then simulated. After that the spherical wave at direction of each element is acquired by interpolation using the spherical coordinates. Finally, the field of spherical wave is added with the *SPAF* to work out the final plane wave on the aperture surface. It's worth mentioning that the proposed compensation approach is a good compromise between accuracy and time, while the full wave computation of the solution region (the feed, array and air between them), occupies huge time and computational resource in large reflectarrays.

2.3. Results Comparison

A reflectarray system example is presented, and the parameters are summarized in Table 1. The configuration is also utilized for the LMDS predesign example subsequently, which is squared cosecant

Table 1. Reflectarray configuration.

Center frequency	13.5 GHz
Position of the feed's phase center	(-140, 0, 300) mm
Element cell dimensions	13 mm \times 13 mm (0.585 λ \times 0.585 λ)
Number of elements	621 (23 \times 27)

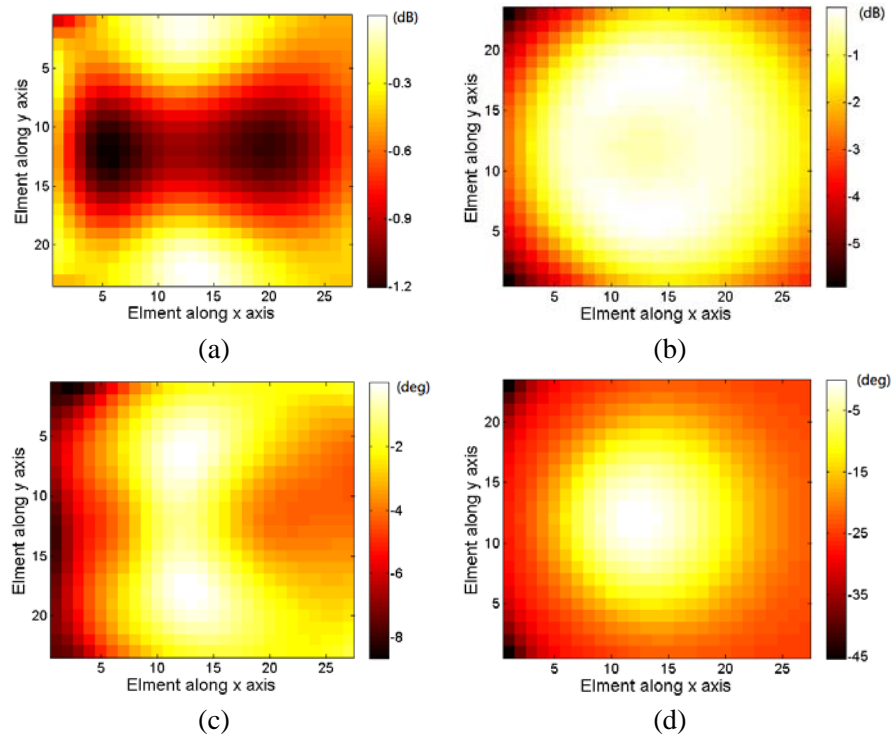


Figure 3. Offset (normalized) between the results of: (a) HFSS and measurement in amplitude; (b) model function and measurement in amplitude; (c) HFSS and measurement in phase; (d) model function and measurement in phase.

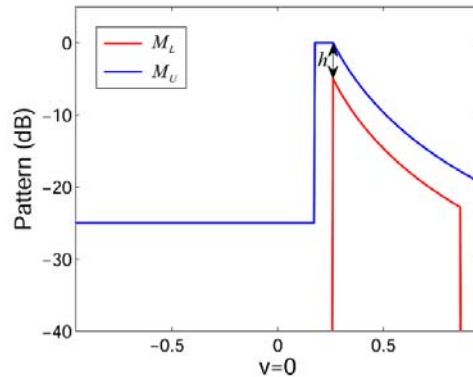


Figure 4. Masks for cosecant squared beam.

in elevation and sectored in azimuth (see Figure 4). The feed is placed away from the broadside to avoid blockage. According to the configuration, the aperture fields calculated by the above-mentioned two approaches are compared with the measured result. As shown in Figure 3, the amplitude and phase offset are compared in dB and degree respectively. The maximum error of the excitation amplitude by local simulation approach is 1.2 dB in Figure 3(a), while it is more than 5 dB by mathematical modeling approach at the edge of the aperture in Figure 3(b). Similarly to amplitude, the maximum phase error calculated by modeling is larger than the local simulation approach apparently, as shown in Figures 3(c) and (d). The distortion becomes severe at the rim of the aperture for the modeling function method. In a word, the incident excitation calculated by local simulation approach is more accurate. Moreover, the

local method cost less time than full-wave method since the feed is isolated solved without considering the reflectarray surface.

3. SYNTHESIS APPROACH WITH NEW CONVERGENCE STRATEGY

As discussed previously, the mathematical modeling approach is lack of accuracy. Nevertheless, the iterating process scarcely converges to global optimum by using the excitation obtained by local simulation approach directly. To avoid local minima for intersection approach without varying the taper of excitation, a new multi-stage convergence strategy is proposed to work with the local simulation approach.

The new proposed multi-stage convergence strategy for intersection approach is described as the gradual variation of the target pattern. This procedure is carried out via varying the desired pattern (i.e., the masks) by a scaling factor α , by which α is varied instead of changing the illumination taper in each step. The α is decided according to the shape of the desired beam, such as the coverage area for contour beam or the offset between M_U (upper mask) and M_L (lower mask) for cosecant squared beam. Specifically, the choice of α is not critical since the intersection approach itself is a robust local optimization algorithm. In brief, the new synthesis process is divided into several steps, during which gradually varied target patterns are set as the realizable patterns (masks). As shown in Figure 4, two masks of cosecant squared beam for LMDS application are taken as an example. The synthesis process begins with a random starting point, the masks easy to optimize ($\alpha > 1$) are chosen so that it is easy to converge at this step. Thereafter, the second step will use the synthesized phase distribution obtained in the previous step as a new starting point, however, a smaller α is set instead. A new phase distribution is then acquired and the process is repeated till $\alpha = 1$ so that the masks will coincide with the specifications of the required pattern at the last step. In addition, phase distribution optimized from each step should be forced symmetric properly according to the demanded pattern shape.

Using the new multi-stage strategy, the optimization procedure is illustrated in the flow chart of Figure 5, consisting of three steps and being specified as follows.

- i. Initialization. Once the configuration of a reflectarray system is specified, the incident field along the vertical and horizontal directions of the unit cell is known as $A^{X/Y}(m, n) \times \Phi_{ini}^{X/Y}(m, n)$, which is calculated by local simulation approach. Besides, elementary reflection property is also analyzed by simulation, and the result should be converted into a data table in the step.
- ii. Optimization. M_U and M_L are defined as required and then h (see Figure 4) is zoomed by a scaling factor α . After that, the intersection approach is employed to optimize the excitation phase by alternating projection between excitation set and target pattern set with the proposed convergence strategy. There exist dual loops in the step, specifically, the internal loop is a projection operation for n cycles, i.e., the box of Intersection Approach in Figure 5. The external loop is the new multi-stage strategy by decreasing α .
- iii. Data processing. The optimized phase distribution $\Phi_{opt.}(m, n)$ is subtracted by the initial phase distribution $\Phi_{ini}^{X/Y}(m, n)$. Thereafter the result is unwrapped into a cycle to calculate the phase delay distribution $\Phi_{comp.}(m, n)$ for compensation. Finally the patch dimensions are obtained by interpolating $\Phi_{comp.}(m, n)$ into the phase data table computed by step 1.

As shown in Figure 5, two judgements are executed during optimization. Firstly, once the loop reaches $\alpha = 1$, the cost measure is calculated by a fitness function defined as

$$\text{Fitness} = \omega_1 \cdot \sum_{\substack{(u,v) \in \text{mainbeam} \\ \text{and } |E(u,v)| < M_L(u,v)}} \sum (|E(u,v) - M_L(u,v)|)^2 + \omega_2 \cdot \sum_{\substack{(u,v) \in \text{mainbeam} \\ \text{and } |E(u,v)| > M_U(u,v)}} \sum (|E(u,v) - M_U(u,v)|)^2, \quad (5)$$

where ω_1 and ω_2 are weight factors for the main lobe and side lobe area. The second satisfactory evaluation is judged artificially after simulation considering the requirements. The former is to evaluate the synthesis result while the latter the simulated result. If the results do not meet the requirements, it means the solution space is too small to converge for the design. The configuration should be redesigned to add more freedoms to reduce the difficulty of convergence.

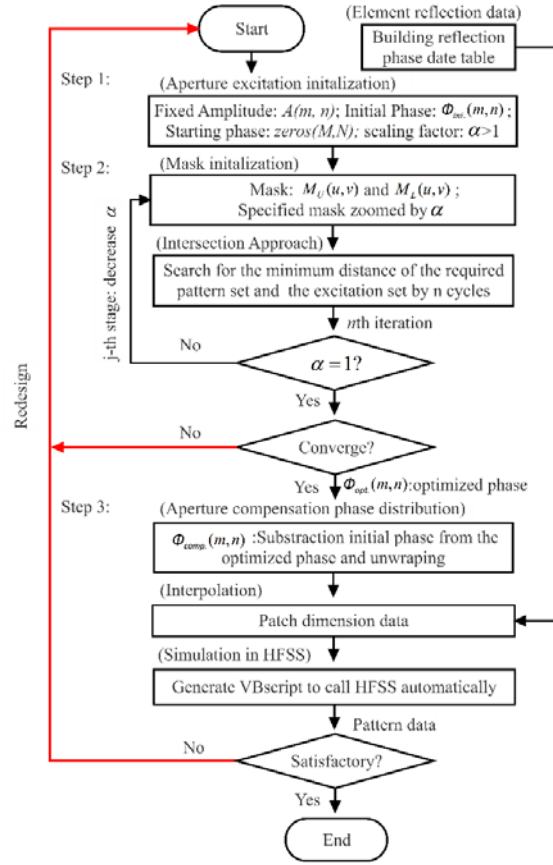


Figure 5. Flow chart of the optimization procedure.

Specifically in the verification process, as all elements are different from each other, one may spend much time of building models for large reflectarrays. Moreover, it is a repeated job if a redesign is necessary. To reduce the model-building time, a co-simulation approach is proposed and added to the design program. We use MATLAB to generate a VBScript to control the HFSS Scripting Interface, by which the 3D model is built and then solved automatically. As shown in Figure 5, once the optimization process is finished, MATLAB will generate a VBScript and then call HFSS to run the VBScript. The co-simulation approach is not only beneficial to reduce the time of designing models, but also connects the optimization and verification operations as a whole.

4. PREDESIGN EXAMPLE

A non-canonical element, consisting of dual concentric varying sized metallic loops printed on a 1 mm-thickness substrate ($\epsilon_r = 2.65$) which is supported by a 3 mm-thickness foamed plastic plate over the ground plane, is adopted for the example. Additionally, the dual-loop structure is arbitrarily chosen instead of the conventional rectangular patch. The reflection coefficient of the element cell is simulated by HFSS, considering the local periodicity.

The patch is enabled to work at 13.5 GHz by optimizing its parameters manually. The lattice dimension is $d_x = d_y = 13$ mm, the width of the two loops 0.5 mm, and the radius ratio between the inner and outer ring $r_{in}/r_{out} = 0.5$, while outside radius is varied from 2 mm to 5 mm. Figure 6 shows the phase curve of the reflection coefficient versus the external radius at the center frequency (13.5 GHz) with normal incidence of a plane wave. The phase curve proves the element available for the design with smoothness phase variation and enough phase range ($> 360^\circ$). In addition, we have also studied the oblique incidence case while the simulations indicate that the phase curve is steady with the incident

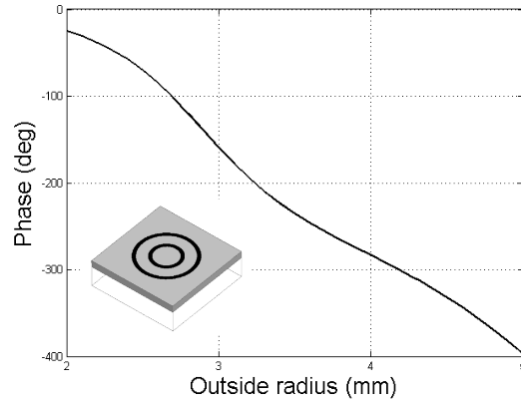


Figure 6. Simulated phase shift versus the radius at the center frequency.

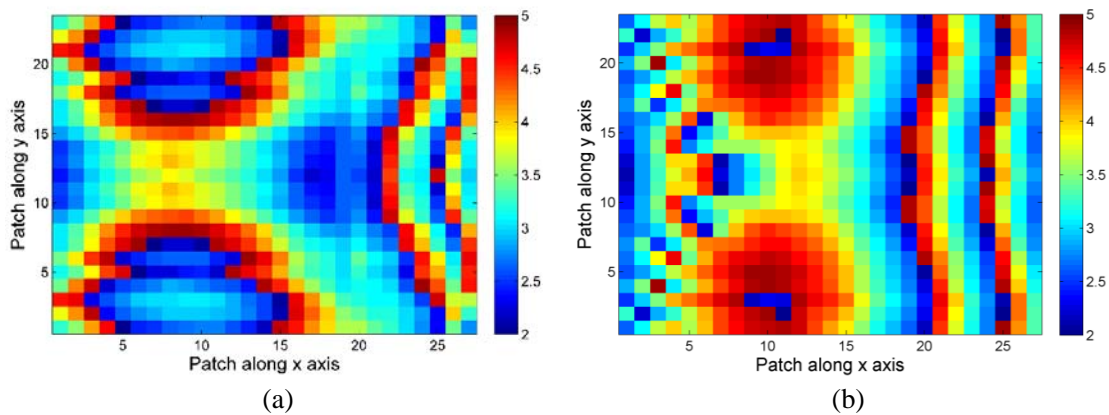


Figure 7. Patch dimensions obtained by (a) proposed strategy and (b) traditional strategy.

angle up to 40° . Hence, the normal incident result is used instead of the oblique one as a compromise since computing the latter costs huge time.

A sectored-cosecant squared beam pattern is analyzed as the target pattern. As shown in Figure 4, the gain of the antenna should be greater than 18 dB for a 55° sectored beam in the azimuth plane, and the pattern is tilted at 15° starting from 10° in the elevation plane. Using the excitation results calculated in Section 2, a $330 \text{ mm} \times 380 \text{ mm}$ reflectarray with 621 elements is determined according to Table 1. After the optimization process with the new convergence strategy, the phase distribution to be compensated is obtained in Figure 7(a), the dimension of each patch is calculated by interpolation using the phase data table in Figure 6. The element dimensions presented in Figure 7(b) are optimized by the traditional convergence strategy for comparison. Two reflectarray models have been built and calculated in HFSS using the two configurations. As can be seen in Figure 8, the simulated pattern optimized by the traditional strategy is severely distorted due to the inaccuracy excitation obtained by modeling function. It is worth noting that the synthesized results of the two strategy are very similar since both of them converge to the optimum despite different excitations. So the synthesized result by the traditional strategy is not plotted in Figure 8 for clear looking. The synthesized and simulated results are in good agreement by the optimization procedure using the new proposed strategy, and both of them meet the requirements very well in the main sectored beam. However, there exists small distortion in the main beam area as well as higher side lobes than expected, which can be attributed to following three reasons. Firstly, the design process of the example is proceeded assuming a normal incidence by the local periodicity approximation. However, the real reflection coefficient of the unit cell beyond the array center is different due to the oblique illumination. Secondly, the discontinuities of adjacent patches leads to some non-uniform coupling. Finally, the pattern is also affected by edge scattering effect.

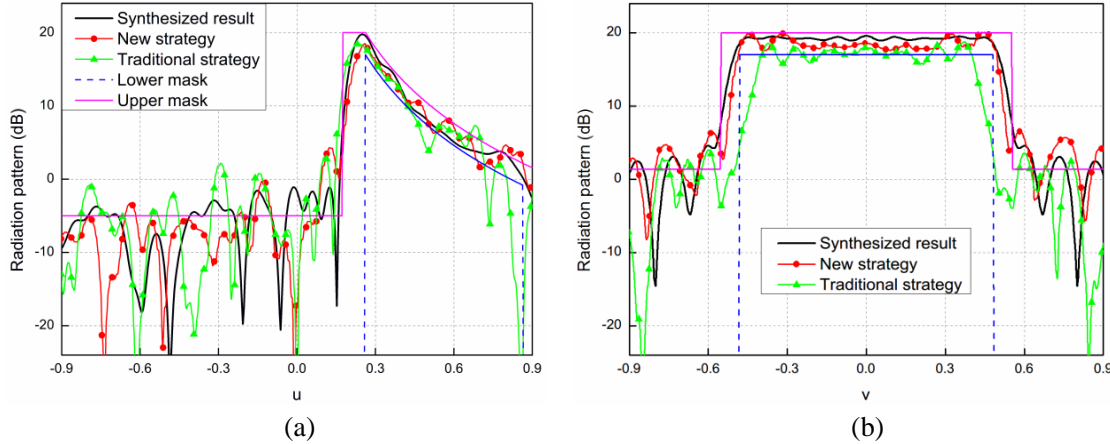


Figure 8. Simulated and synthesized radiation patterns in (a) elevation plane and (b) azimuth plane.

The optimization program consumes 25.6 seconds with 440 iterations on personal computer (i5-2500K, 4 Gigabyte RAM), compared to 45.992328 seconds with 650 iterations by the traditional method. The total reflectarray system is simulated in HFSS v15 executed by VBScript. Thanks to the FE-BI boundary condition, the problem area is dramatically reduced, which makes the computing time less than an hour on the platform of HP workstation Z800 (72 Gigabyte RAM).

5. CONCLUSION

An improved predesign procedure for shaped-beam reflectarrays is discussed in this paper. A local simulation approach has been developed to calculate the excitation distribution, which is a good compromise between accuracy and time. Cooperating with the local simulation approach, a new multi-stage convergence strategy has been proposed to avoid local minima. Moreover, a co-simulation approach has been achieved by combining the optimization and simulation together using VBScript, which can save a lot of time for building reflectarray models instead of manual operation. The predesign of a 621-element sectored-cosecant squared beam reflectarray is presented as an example. The results validate the approach and demonstrate the potential for shaped-beam reflectarray applications.

REFERENCES

1. Huang, J., *Reflectarray Antenna*, Wiley Online Library, 2008.
2. Chaharmir, M. R., et al., "Design of broadband, single layer dual-band large reflectarray using multi open loop elements," *IEEE Transactions on Antennas and Propagation*, Vol. 58, No. 9, 2875–2883, 2010.
3. Chulmin, H., et al., "A high efficiency offset-fed X/Ka-dual-band reflectarray using thin membranes," *IEEE Transactions on Antennas and Propagation*, Vol. 53, No. 9, 2792–2798, 2005, 10.1109/TAP.2005.854531*10.1109/TAP.2005.854531.
4. Arrebola, M., et al., "Multifed printed reflectarray with three simultaneous shaped beams for LMDS central station antenna," *IEEE Transactions on Antennas and Propagation*, Vol. 56, No. 6, 1518–1527, 2008.
5. Encinar, J. A., et al., "A transmit-receive reflectarray antenna for direct broadcast satellite applications," *IEEE Transactions on Antennas and Propagation*, Vol. 59, No. 9, 3255–3264, 2011.
6. Nayeri, P., et al., "Design and experiment of a single-feed quad-beam reflectarray antenna," *IEEE Transactions on Antennas and Propagation*, Vol. 60, No. 2, 1166–1171, 2012.
7. Bucci, O. M., et al., "Intersection approach to array pattern synthesis," *IEE Proceedings H — Microwaves, Antennas and Propagation*, Vol. 137, No. 6, 349–357, 1990.

8. Nayeri, P., et al., "Design of single-feed reflectarray antennas with asymmetric multiple beams using the particle swarm optimization method," *IEEE Transactions on Antennas and Propagation*, Vol. 61, No. 9, 4598–4605, 2013, 10.1109/TAP.2013.2268243*10.1109/TAP.2013.2268243.
9. Zornoza, J. A. and J. A. Encinar, "Efficient phase-only synthesis of contoured-beam patterns for very large reflectarrays," *Int. J. RF and Microwave Computer-Aided Engineering*, Vol. 14, No. 5, 415–423, 2004.
10. Encinar, J. A. and J. A. Zornoza, "Three-layer printed reflectarrays for contoured beam space applications," *IEEE Transactions on Antennas and Propagation*, Vol. 52, No. 5, 1138–1148, 2004.
11. Leberer, R. and W. Menzel, "A dual planar reflectarray with synthesized phase and amplitude distribution," *IEEE Transactions on Antennas and Propagation*, Vol. 53, No. 11, 3534–3539, 2005.
12. Vescovo, R., "Reconfigurability and beam scanning with phase-only control for antenna arrays," *IEEE Transactions on Antennas and Propagation*, Vol. 56, No. 6, 1555–1565, 2008.
13. Changhua, W. and J. A. Encinar, "Efficient computation of generalized scattering matrix for analyzing multilayered periodic structure," *IEEE Transactions on Antennas and Propagation*, Vol. 43, No. 11, 1233–1242, 1995, 10.1109/TAP.1995.481174*10.1109/TAP.1995.481174.
14. Carrasco, E., et al., "Design, manufacture and test of a low-cost shaped-beam reflectarray using a single layer of varying-sized printed dipoles," *IEEE Transactions on Antennas and Propagation*, Vol. 61, No. 6, 3077–3085, 2013.
15. Carrasco, E., et al., "Demonstration of a shaped beam reflectarray using aperture-coupled delay lines for LMDS central station antenna," *IEEE Transactions on Antennas and Propagation*, Vol. 56, No. 10, 3103–3111, 2008.
16. Arrebola, M., et al., "Multifed printed reflectarray with three simultaneous shaped beams for LMDS central station antenna," *IEEE Transactions on Antennas and Propagation*, Vol. 56, No. 6, 1518–1527, 2008.